The self-assembly and thermoresponsivity of poly(isoprene-*b*-methyl methacrylate) copolymers in non-polar solvents

Daniel M. Day and Lian R. Hutchings*

Durham Centre for Soft Matter, Department of Chemistry, Durham University, Durham, DH1 3LE, United Kingdom.

ABSTRACT. The self-assembly of a series of polyisoprene-*block*-poly(methyl methacrylate) (PI-*b*-PMMA) block copolymers, in aliphatic hydrocarbon solvents is reported for the first time. The block copolymers were prepared by a change of mechanism polymerisation (CHOMP) whereby living anionic polymerisation was used to prepare polyisoprene macroinitiators for ATRP (PI-Br), which was in turn used to polymerize MMA. The use of anionic polymerisation ensured optimal control over the molar mass and dispersity of the polyisoprene block, in a synthesis that is readily scaled-up, to enable the production of homologous series of block copolymers by varying only the molar mass of the PMMA block. The block copolymers were subsequently dispersed in *n*-decane or *n*-hexane, a selective solvent for the PI block at high solids content of up to 30 wt%. Analysis of the resulting self-assembled nanostructures using DLS and TEM revealed that the block copolymers self-assemble into varying morphologies (spherical micelles, wormlike micelles or vesicles), dependent upon the molar mass and composition of the block copolymer, enabling the

construction of a series of "phase-diagrams". The resultant self-assembled structures were also found to be thermally responsive and, in some cases, underwent a change in morphology upon heating.

INTRODUCTION

The self-assembly of block copolymers (BCPs) can be traced back to the 1960s[1, 2] following the discovery of living anionic polymerisation by Szwarc, in the previous decade.[3] In the 1980s Bahadur *et al*. reported the micellar behaviour of poly(styrene-*b*-isoprene) BCPs in solvents which are either selective for the styrene or the isoprene block [4] and more recently Hadjichristidis demonstrated the versatility and control afforded by anionic polymerisation by synthesizing a series of compositionally (nearly) identical copolymers of styrene and isoprene, which varied in the distribution of the two monomers along the chain.[5] Thus, copolymers with block, tapered, inverse-tapered and random arrangements of monomers were made and their self-assembly in *n*-decane investigated. Whilst living anionic polymerisation (LAP) is the optimal technique for imparting control over molar mass, dispersity and in many cases monomer sequence, LAP is extremely restricted in terms of suitable monomers. Whilst it is possible to polymerise methyl methacrylate (and other methacrylates) *via* LAP, to do so with control requires a number of well-documented challenges to be overcome.[6-8] These include side-reactions between the carbanion and the carbonyl functionality of the methacrylate ester, during both initiation and propagation steps.[9, 10] These challenges can be overcome by a combination of bulky initiators with reduced nucleophilicity, the use of polar solvents and/or lithium salt additives and reduced reaction temperatures.[11-14] However, the development of reversible deactivation radical polymerisation (RDRP) mechanisms over the past 25 years has enabled the facile synthesis of polymers and

copolymers comprising of (meth)acrylate monomers and in many cases block copolymers for self-assembly.[15-17]

The self-assembly of BCPs, when dispersed in a selective solvent for one of the constituent blocks, continues to be a widely studied field and self-assembly of amphiphilic BCPs into micellar structures in aqueous media has been widely reported with potential applications including drug delivery, coatings and lithography. [18-22] Such BCPs contain a polar, hydrophilic block, and are commonly prepared entirely by (RDRP) or frequently by using a poly(ethylene oxide) macroinitiator for the RDRP of a hydrophobic block.[23, 24] Amphiphilic BCPs are widely exploited by industry with perhaps the most well-known class being ABA triblock copolymers of poly(ethylene oxide)-*b*-poly(propylene oxide)-*b*-poly(ethylene oxide) (PEO-*b*-PPO-*b*-PEO), also known as Pluronics or Polyoxamers – their self-assembly in aqueous solution has been frequently reported and reviewed.[25]

In contrast, aside from the historical interest in the self-assembly of BCPs prepared by anionic polymerisation mentioned above, there are significantly fewer recent reports of BCPs which self-assemble in non-polar organic solvents. However, notable contributions have been reported recently by Armes *et al.* [26-30] who have reported polymerisation induced self-assembly (PISA) in aliphatic hydrocarbons, predominantly exploiting RAFT polymerisation of long-chain acrylates/methacrylates as the lipophilic, oil-soluble, corona-forming block and a shorter, insoluble acrylate/methacrylate as the core-forming block. PISA undoubtedly offers significant benefits and RAFT dispersion polymerisation can be carried out under benign conditions and at high solids content whilst maintaining a low solution viscosity. However, the monomers used are often relatively expensive, creating an additional challenge for commercially viable, industrial-scale production. Moreover, PISA is not necessarily a pre-requisite for the synthesis of such BCPs

and a solution-based approach is equally viable.[31] In such cases the resultant BCPs can be dispersed from solution by the addition of a selective non-solvent to drive self-assembly.[32, 33]

Isoprene is an example of a class of monomers (dienes) of significant industrial relevance. However, well-documented difficulties in the polymerisation of dienes by RDRP mechanisms have prevented detailed investigations of the self-assembly of BCPs comprising a diene block,[34, 35] the like of which have been reported for BCPs that are more easily prepared by e.g. PISA. In the current work, the advantages of using LAP for the facile and well-controlled polymerisation of isoprene, are combined with benefits of using ATRP, an equally facile and reasonably well-controlled mechanism for the polymerisation of methacrylate monomers.

The concept of mechanism transformation polymerization is not new, and was first reported by Acar *et al.* in 1999.[36] The general procedure was termed as 'Change of Mechanism Polymerisation' (CHOMP) later in the same year by Hillmyer, who described the concept as an opportunity to significantly expand the range of available block copolymers by the combination of two distinct polymerisation mechanisms, to produce block copolymers comprising of "mechanistically incompatible segments".[37] This approach has subsequently been adopted by us and others.[38-41] In the context of the current work a CHOMP approach was chosen because the desired block copolymers comprised not so much of "mechanistically incompatible" blocks as much as mechanistically challenging blocks. It *is* possible to make PMMA by LAP, although due to the challenges alluded to above, it is far easier to use ATRP. Likewise, it is not impossible to synthesise polyisoprene by an RDRP mechanism, but for this monomer RDRP is just not as effective as LAP.[35, 42-47] Whilst there are reports of the "successful" polymerisation of isoprene and butadiene by RDRP, the dispersity and control of molar mass are without exception significantly worse than what is routinely possible with LAP.[34, 48, 49]

Very recently Armes described a CHOMP approach in which a single sample of hydroxyl-terminated hydrogenated polybutadiene (prepared by anionic polymerisation of butadiene) was transformed into a macro CTA for the RAFT PISA of benzyl methacrylate (BA) in *n*-dodecane.[50] A series of BCPs were produced with a fixed block-length of hydrogenated polybutadiene (hPBD) and blocks of PBA of varying degree of polymerisation (DP), allowing the construction of a phase diagram. Perhaps unexpectedly, only spherical micelles were observed for PBA with DPs of up to 300 at 25 wt% solids content and large parts of the phase diagram were populated by mixed phases, with worms and (polydisperse) vesicles only observed at high solids content and/or high DP.

In the present work, polyisoprene samples of varying molar mass have been used to prepared multiple series of poly(isoprene-*block*-methyl methacrylate) (PI-*b*-PMMA) BPCs. In each series, by fixing the molar mass of the polyisoprene block and systematically varying the molar mass of the PMMA block, homologous series of block copolymers were produced. The resulting block copolymers were recovered from solution and induced to undergo post-polymerisation self-assembly by a commonly-used solvent-switching technique, where the block copolymer is dissolved in a good solvent for both blocks before being added to the selective solvent.[51, 52] When dispersed in *n*-decane, a solvent that is selective for the polyisoprene block, the block copolymers undergo self-assembly allowing a detailed mapping of the impact of both core- and corona-forming block length, BCP composition and solids content on self-assembled morphology. The full range of expected self-assembled nanostructures were observed including spherical and worm-like micelles and vesicles. The different nanostructures were characterised/identified by DLS and TEM and the thermoresponsivity of the self-assembled structures was investigated by rheology.

EXPERIMENTAL

MATERIALS

Isoprene (Sigma-Aldrich; 99 %, containing <1000 ppm *p*-TBC), toluene (Fisher; ≥99.9 %), dichloromethane (Fisher; ≥99.8 %) and benzene were dried with calcium hydride (Acros; ca. 93 %, 0-2 mm grain size) and degassed by a series of freeze-pump-thaw cycles. 1,4-Dioxane (Fisher; ≥99 %) and methyl methacrylate (Sigma-Aldrich; 99 %, containing ≤ 30 ppm MEHQ) were each passed through neutral aluminium oxide (Fisher; Brockmann l, 60 Å) before use. *Sec*-Butyllithium (Sigma-Aldrich; 1.4 M in cyclohexane), butylated hydroxytoluene (Sigma-Aldrich; ≥99 %), chloroform-*d* (Apollo; 99.96 atom% D), *α*-bromoisobutyryl bromide (Sigma-Aldrich; 98 %), methanol (Fisher; AR grade), triethylamine (Sigma-Aldrich; 99.5 %), copper (I) bromide (Acros; 98 %, extra pure), 2-2'-bipyridyl (Sigma-Aldrich; ≥99 %) and *n*-decane (Fisher; >99 %) were all used as received. Ethylene oxide (Sigma-Aldrich; ≥99.5 %) was dried and purified by passing through columns of Carbosorb (Sigma-Aldrich) and further dried and purified by stirring for 30 minutes at 0 °C over calcium hydride. The gaseous monomer was further purified by treatment with *n*-butyllithium (Sigma-Aldrich; 2.5 M in hexanes) immediately prior to use.

CHARACTERISATION

Molar mass analysis was carried out by size exclusion chromatography (SEC) using a Viscotek TDA 302 with detectors for refractive index, light scattering and viscosity. Two 300 mm PLgel 5 µm mixed C columns were used with a linear molecular weight range of $200 – 2\,000\,000$ g mol^{-1}. THF was used as the eluent at a flow rate of 1.0 mL min^{-1} at a temperature of 35 °C. For all polymers, triple detection SEC was utilised for molar mass determination with light scattering, using values of 0.085 mL g^{-1} for poly(methyl methacrylate) (PMMA) and 0.130 mL g^{-1} for

polyisoprene (PI). Samples were prepared for SEC analysis by dissolving c. 2 mg of the polymer in 2 mL THF for a concentration of c. 1 mg mL^{-1}.

Proton NMR spectra were recorded using a Bruker DRX-400 (400 MHz, 298 K) spectrometer with chloroform-*d* as the solvent. The trace of non-deuterated chloroform present in the solvent was used to reference the spectra (7.26 ppm).

Rheological characterisation of self-supporting gels was performed using a TA AR-2000 rheometer, equipped with a 25 mm parallel plate geometry and a Peltier plate for thermal analysis. Free-flowing liquids were analysed in the same way, but with a concentric cylinder geometry. Angular frequency (ω) sweeps were conducted at 25 °C and from these, a constant angular frequency of 1 rad s^{-1} and strain of 0.2 were used for the temperature sweep experiments. Complex viscosity (η*) was calculated from: $\eta^* = \frac{\sqrt{G'^2 + G''^2}}{\omega}$

High resolution transmission electron microscopy (TEM) images were obtained using a JEOL 2100F FEG TEM operating at 200 kV. For free-flowing copolymer morphologies, holey carbon grids (Agar scientific; holey carbon film on 300 mesh copper grids) were dipped in the liquid polymer dispersion, prepared at 15 wt% in decane (or 0.1 wt% for the diluted samples) and blotted with filter paper to remove the excess solvent. For self-supporting gels, a thin film was spread on a glass slide, onto which the holey carbon grid was dipped and blotted on filter paper.

Particle size analysis of self-assembled structures was carried out using a Malvern Panalytical Zetasizer μV (scattering angle θ = 90°). Values reported herein are the intensity-average hydrodynamic diameter with the PDI obtained using the cumulant analysis embedded in the software. Samples were prepared by dispersion of polymer samples at 15 wt% in *n*-decane, followed by dilution with decane to 0.72 wt%. Dispersions in *n*-decane (≈1 mL) were added to a

1 cm quartz cuvette, by injection through a 0.2 μm PTFE syringe filter. Each experiment was repeated three times with 13 measurements recorded in each case.

POLYMER SYNTHESIS

Ethylene Oxide-end-capped Polyisoprene (PI-*OH*)

Living anionic polymerisation was employed to prepare a series of polyisoprene ATRP macroinitiators, of varying molar mass, using standard high vacuum techniques and trap to trap distillation. Thus, in a typical reaction, the synthesis of PI-*OH* with a target molar mass of 3500 g mol^{-1} was carried out as follows: toluene (≈50 mL) and isoprene (8.1 g, 120 mmol) were distilled into the reactor. *s*-BuLi (1.4 M in cyclohexane; 1.64 mL, 2.3 mmol) was injected via rubber septum, causing the reaction mixture to turn pale yellow. The propagation of isoprene was allowed to proceed with stirring at room temperature for 2 hours. Meanwhile, ethylene oxide (1.1 mL; 0.97 g, 22 mmol) was distilled onto calcium hydride and stirred for 30 minutes, cooled to 0 °C with an ice-water bath. The EO was then distilled into the reactor, causing the contents to turn colourless within 1 minute of stirring. The reaction was left overnight to ensure quantitative end-capping before the reaction was terminated by the addition of a 1:1 HCl (37 wt% in water)/methanol by volume for an HCl concentration of 6 M (0.38 mL, 2.3 mmol). The polymer was recovered by addition of the polymer solution to 400 mL of methanol. The viscous liquid polymer was allowed to settle before the supernatant liquor was decanted to yield a colourless, sticky viscous liquid, which was dried in vacuo to constant mass to yield PI$_{55}$-*OH* (6.7 g, 83 %). The polymer was stored in a freezer until further use. SEC: M_n (PI$_{55}$-*OH*) = 3730 g mol^{-1}, M_w = 3880 g mol^{-1}; M_w/M_n = 1.04. Proton NMR (400 MHz, CDCl$_3$, 298 K, ppm): δ = 1.62-1.70 CH$_2$-CH=C(**CH$_3$**)-CH$_2$), 1.90-2.07 (**CH$_2$**-CH=C(CH$_3$)-**CH$_2$**), 2.38 (-**CH$_2$**-CH$_2$-OH), 3.51 (-CH$_2$-**CH$_2$**-OH), 3.63 (-CH$_2$-CH$_2$-**OH**), 4.67-5.15 (CH$_2$-**CH**=C(CH$_3$)-CH$_2$).

Bromide-end-capped Polyisoprene (PI-Br)

The hydroxyl end-capped PI$_{55}$-*OH* was converted to an ATRP macroinitiator according to the following procedure: PI$_{55}$-*OH* (3730 g mol^{-1}) (6.0 g, 1.6 mmol) was charged to a Schlenk flask containing a magnetic stirrer bar, which was sealed with a rubber septum and placed under high vacuum. Dichloromethane ($\approx$30 mL) was then distilled into the flask. The temperature was lowered to 0 °C, before the injection of triethylamine (0.67 mL; 0.49 g, 4.8 mmol) and α-bromoisobutyryl bromide (0.60 mL; 1.11 g, 4.8 mmol) via rubber septum. After 3 hours at 0 °C, the reaction mixture (which had turned pale brown) was warmed to room temperature and left stirring. After 18 hours, the contents had turned dark brown. The polymer was precipitated by addition of the polymer solution to 400 mL methanol. The viscous liquid polymer was allowed to settle before being recovered by pouring off the supernatant liquor to yield a clear, brown, sticky viscous liquid. PI$_{55}$-Br (5.1 g, 81 %). SEC: M_n = 3710 g mol^{-1}; M_w = 3860 g mol^{-1}; M_w/M_n = 1.04. Proton NMR (400 MHz, CDCl$_3$, 298 K, ppm): δ = 1.62-1.70 CH$_2$-CH=C(**CH$_3$**)-CH$_2$), 1.95 (C(**CH$_3$**)$_2$), 1.90-2.07 (**CH$_2$**-CH=C(CH$_3$)-**CH$_2$**), 4.67-5.15 (CH$_2$-**CH**=C(CH$_3$)-CH$_2$).

Preparation of PI-*b*-PMMA

The following describes a typical procedure for the preparation of PI-*b*-PMMA samples by ATRP. Thus in a typical reaction, for a target molar mass of PMMA of 25000 g mol^{-1}, PI$_{55}$-Br (3710 g mol^{-1}; 0.38 g, 0.10 mmol) and 2,2'-bipyridyl (66 mg, 0.42 mmol) were charged to a Schlenk flask which was sealed with a rubber septum. MMA (2.55 g, 25 mmol) and 1,4-dioxane ($\approx$10 mL) were charged to the flask, after passing through columns of neutral aluminium oxide immediately prior to use. The contents were then degassed by freeze-pump-thaw cycles before raising to atmospheric pressure with nitrogen gas. Meanwhile, copper (I) bromide (17 mg, 0.12 mmol) was charged to a separate Schlenk flask, containing a magnetic stirrer bar, which was sealed

with a rubber septum. This was evacuated and back-filled with nitrogen gas 3 times to remove any oxygen. The dioxane solution of macroinitiator, monomer and ligand was then added to the copper bromide by injection via a rubber septum before the mixture was degassed via freeze-pump-thaw cycles. The flask was raised to atmospheric pressure with nitrogen and the mixture stirred magnetically overnight at 90 °C. The following morning, the contents had turned green, indicating the presence of copper (II) salts. The solution was cooled to room temperature, passed through a column of neutral aluminium oxide to remove the copper salts and the copolymer recovered by addition to 250 mL methanol containing BHT (≈5000 mg). The precipitated polymer was collected by filtration to yield a white powder. PI_{55}-b-$PMMA_{192}$ (2.3 g, 79 %).

Proton NMR (400 MHz, $CDCl_3$, 298 K, ppm): δ = 0.86-1.15 (-**CH₃**), 1.62-1.69 **CH₂**-CH=C(CH₃)-**CH₂**), 1.83 (-**CH₂**), 1.90-2.05 (**CH₂**-CH=C(CH₃)-**CH₂**), 3.61 (-O-**CH₃**), 4.67-5.14 (**CH₂**-**CH**=C(CH₃)-**CH₂**).

SEC: M_n = 23,000 g mol^{-1}; M_w = 31,900 g mol^{-1}; M_w/M_n = 1.29.

Self-Assembly of Block Copolymers in *n*-Decane

The self-assembly of the PI-*b*-PMMA in *n*-decane is exemplified as follows. PI_{32}-*b*-$PMMA_{73}$ (1.00 g) was dissolved in dichloromethane (6.50 g) in a vial with magnetic stirring, to give a colourless solution. Meanwhile, *n*-decane (0.50 g) was weighed into a separate vial, containing a magnetic stirrer. The required amount of block copolymer solution (see Table S1 for mass of solution added for each sample) was added dropwise to the *n*-decane (0.50 g) with rapid stirring. The slightly turbid solution was then heated to 60 °C with magnetic stirring to evaporate DCM until the mass of solution reached that of *n*-decane plus added polymer.

RESULTS AND DISCUSSION

A two-step CHOMP approach was adopted for the synthesis of PI-*b*-PMMA BCPs. In the first step, LAP was used to produced ethylene oxide end-capped polyisoprene (PI-*OH*) which, following conversion to an ATRP macroinitiator (PI-Br), was used for the polymerisation of MMA by ATRP. Although, as mentioned above, it is possible to prepare PI-*b*-PMMA block copolymers solely by anionic polymerisation, the CHOMP approached was adopted in the current work to ensure that the molar mass of the PI block was identical in each homologous series of PI-*b*-PMMA block copolymers.

Synthesis of Poly(isoprene-*block*-(methyl methacrylate)) (PI-*b*-PMMA)

Ethylene oxide end-capped polyisoprene (PI-*OH*) was prepared by living anionic polymerisation according to a previously published method and illustrated in Scheme S1.[53] Error! Reference source not found.Ethylene oxide was used in (at least) a 10-fold excess with respect to *s*-BuLi to ensure quantitative end-capping, in the knowledge that ethylene oxide is unable to propagate when using a lithium counter-ion.[54] A series of 3 PI-*OH* polymers with different molar mass were synthesised (see Table S2). In all cases the molar mass obtained by SEC was in excellent agreement with the predicted values and dispersities were low. A characteristic proton NMR spectrum for ethylene oxide end-capped polyisoprene is shown in Figure S1. By comparing the integration values of the peaks at $\delta 3.56 - 3.79$ ppm representing the CH_2 adjacent to the hydroxyl end-group with those of polyisoprene, the degree of end-capping can be calculated to be 100 %. This is consistent with reports in the literature which suggests the reaction of living polystyryl lithium in benzene reacts quantitatively with ethylene oxide.[55]

In order to prepare an ATRP macroinitiator, bromoacetylation of PI-*OH* was carried out using an excess of α-bromoisobutyryl bromide in the presence of triethylamine, in a similar fashion to

previous reports.[56] The proton NMR spectrum of the bromide-end-capped polyisoprene (PI-Br) macroinitiator is shown in Figure S2.**Error! Reference source not found.** The emergence of a peak at δ1.95 ppm is characteristic of the methyl groups (highlighted in pink) introduced following end-capping with bromoisobutyryl bromide. It is not possible to ascertain precisely the degree of end-capping using this peak because of overlap with the peak of the protons adjacent to the double bond of polyisoprene (highlighted in green). However, the success of this reaction is also indicated by the total disappearance of the C**H**$_2$-*OH* peak at δ3.56 – 3.79 ppm, to be replaced by a new peak at δ4.05 – 4.21 ppm following conversion to an ester (highlighted in red). The degree of esterification was calculated to be approximately 100% by comparing the integrals of the peak at δ4.05 – 4.21 ppm with those of polyisoprene. However, it should be noted that the peak in question, arising from an end-group is not intense and the integral value will be subject to an error. An approximately 100% degree of esterification was also calculated for the other macroinitiators prepared in this study .

The copper-catalysed ATRP of MMA has been widely reported using a range of conditions and a variety of initiators, ligands, solvents etc.[57-62] For this study, a system with copper (I) bromide catalyst, 2,2-bipyridyl ligand and 1,4-dioxane as the solvent, at 90 ºC was used to prepare (PI-*b*-PMMA). Molar mass analysis for the BCPs was carried out using a combination of SEC and NMR and the data for all BCPs prepared in this study are reported in Table 1. Exemplar SEC chromatograms for PI$_{55}$-Br and the respective PI$_{55}$-*b*-PMMA$_x$ block copolymers are shown in Figure S3. The chromatograms for all PI-*b*-PMMA block copolymers show a significant shift to lower retention volumes (higher molar mass) for the block copolymers compared to the respective PI-Br macroinitiator. This is entirely in line with expectations for a successful block copolymer synthesis. It is also clear from the chromatograms and the data in Table 1 that the dispersity values

for the block copolymers are higher than that of the precursor macroinitiator. This is not unexpected given that termination reactions may still occur in ATRP reactions and ATRP routinely results in broader molar mass distributions than LAP.

Table 1. Molar mass data for PI_x-b-$PMMA_y$ block copolymers where x and y are degree of polymerisation obtained by SEC for PI block and NMR for PMMA block respectively.

Sample Name	M_n(theo)[a] / g mol^{-1}	M_n(expt) / g mol^{-1}	M_n (NMR)[b] / g mol^{-1}	Đ
PI_{32}	2040	2150	-	1.07
PI_{32}-b-$PMMA_{71}$	22000	15100	9290	1.19
PI_{32}-b-$PMMA_{73}$	9540	11700	9460	1.50
PI_{32}-b-$PMMA_{96}$	14500	13300	11800	1.48
PI_{32}-b-$PMMA_{107}$	12000	15500	12900	1.46
PI_{32}-b-$PMMA_{161}$	22200	22700	18300	1.24
PI_{55}	3540	3730	-	1.04
PI_{55}-b-$PMMA_{53}$	8540	11400	9060	1.29
PI_{55}-b-$PMMA_{74}$	11000	12200	11100	1.31
PI_{55}-b-$PMMA_{183}$	23500	20400	22100	1.21
PI_{55}-b-$PMMA_{192}$	28500	24700	23000	1.29
PI_{55}-b-$PMMA_{347}$	38500	29600	38500	1.27
PI_{74}	5040	5030	-	1.06
PI_{74}-b-$PMMA_{69}$	25000	15100	11900	1.19
PI_{74}-b-$PMMA_{154}$	75000	24000	20400	1.21
PI_{74}-b-$PMMA_{169}$	45000	28200	22000	1.22
PI_{74}-b-$PMMA_{172}$	30000	25100	22200	1.26
PI_{74}-b-$PMMA_{198}$	35000	29000	24900	1.26
PI_{74}-b-$PMMA_{233}$	50000	30700	28400	1.35
PI_{74}-b-$PMMA_{250}$	40000	33000	30100	1.38
PI_{74}-b-$PMMA_{356}$	70000	54700	41000	1.19
PI_{74}-b-$PMMA_{467}$	95000	50400	51800	1.39

[a] Molar mass PI + theoretical molar mass of PMMA

It is worth noting that the chromatograms in Figure S3 for the PI_{55} series, and specifically for PMMA blocks with a low DP, contain a small shoulder, at a retention volume which is coincident with the peak corresponding to the macroinitiator, indicating the presence of residual polyisoprene homopolymer in the final product. The proton NMR spectrum (Figure S2) for PI-Br macroinitiator suggests approximately 100% end-capping of polyisoprene with the initiating bromide moiety, therefore the most likely reason for the presence of PI in the SEC trace is a slow rate of initiation by PI-Br in the ATRP of MMA. This may explain why the shoulder does not appear for the block copolymers with a higher DP_{PMMA}. It is also noteworthy that the dispersity is rather high, even for ATRP, with values approaching 1.5 for some of the PI_{32} series. In these cases the SEC chromatograms also indicate the presence of residual polyisoprene homopolymer, again suggesting a slow rate of re-initiation from the macroinitiator. In these cases, perhaps the dispersity values are higher than for the PI_{55} series because the molar mass of the macroinitiator is lower, increasing the difference in molar mass between (unreacted) macroinitiator and block copolymer. The SEC chromatograms of the relevant PI_{32}-*b*-PMMA block copolymers are shown in Figure S4).

It is clear from the molar mass data in Table 2 that there is a discrepancy between the molar mass obtained from NMR data and the molar mass obtained by SEC. Triple detection SEC analysis requires the use of an accurate value for the refractive index increment (dn/dc), which varies according to the polymer. In the current study a dn/dc value of 0.085 mL g^{-1} was used, which is the dn/dc of PMMA. Thus, an error will be expected for a block copolymer, which is particularly evident when the PMMA block is shorter. For this reason, we believe that the molar mass of the copolymers in this study is more accurately determined using NMR data, also reported in Table 2. A typical NMR spectrum for a PI-*b*-PMMA block copolymer is included as supporting information

(Figure S5) which is accompanied by an explanation of the method used for calculating the molar mass of the PMMA block.

SELF-ASSEMBLY OF PI-*b*-PMMA BLOCK COPOLYMERS IN *n*-ALKANES

Recently, polymerisation-induced self-assembly (PISA) has been widely reported, predominantly using RAFT polymerisation.[57, 63, 64] Whilst there are many benefits of this technique, including relative simplicity and scalability, there are also associated difficulties such as purification of the subsequently self-assembled block copolymer.[65] However, PISA is not the only viable process to enable BCPs to self-assemble. In the current study, BCPs were dissolved in a common solvent and subsequently exposed to a solvent switching method (i.e. by evaporation) to drive self-assembly, as has been described in the literature.[32, 66, 67] Thus, a solution of the block copolymer in dichloromethane was typically added dropwise into *n*-decane, a selective solvent for the PI block, with rapid stirring, before evaporation of the common solvent (DCM). The self-assembly of three homologous series of PI-*b*-PMMA BCPs was studied. In each series the molar mass of the PI-block remains constant and the molar mass of the PMMA block is systematically varied. Each BCP was dispersed at a variety of concentrations, from 5 – 30 wt%, resulting in the formation of stable nanoparticle dispersions. It is notable that this was possible even for solids contents as high as 30 wt% by the post-polymerisation, solvent-switching process! Self-assembly of block copolymers up to 50 wt% has previously been discussed as a significant benefit of the RAFT-mediated PISA process.[28, 65] Three distinctive self-assembled nanostructures were observed, which manifested themselves as free-flowing liquids, transparent gels and opaque gels, depending on the molar mass of the PMMA block and/or solids content. These are shown in a "phase diagram" below for BCPs based on the PI_{32}-Br macroinitiator (**Error! Reference source not found.**d). Phase diagrams for the PI-*b*-PMMA block copolymers prepared from PI_{55}-Br and

PI$_{74}$-Br macroinitiators, dispersed in *n*-hexane and *n*-decane respectively, are included as supporting information in Figure S6.

The phase diagram in **Error! Reference source not found.**d shows that for PI-*b*-PMMA block copolymers formed from PI$_{32}$-Br, with a PMMA block of DP < 73, the self-assembled structures form free-flowing liquids at all solids contents up to 30 wt%. It is also clear that at 5 wt%, all BCPs in this series self-assemble into free-flowing liquids, regardless of the DP of the PMMA block. However, at 10 wt% (and above), the BCP with PMMA DP = 86 formed self-supporting transparent gels and as the PMMA block DP increases to 161, self-supporting opaque gels were observed above 10 wt% solids content. The impact of molar mass, composition and solids content on the self-assembly of BCPs prepared via PISA has been represented in similar phase diagrams in previously published reports[21, 26, 68, 69] which also discuss the different self-assembled morphologies that give rise to the various physical behaviors. Transmission electron microscopy (TEM) and dynamic light scattering (DLS) are commonly utilised to identify and measure the particle sizes of self-assembled morphologies and the reports cited above describe the presence of mixed phases where different morphologies appear in the same solution. However it is not entirely clear whether this is caused by dispersity in block length resulting in BCPs samples which span the phase boundaries. Mixed phases are particularly common at lower dispersion concentrations because, for example, the spherical micelles have a decreased likelihood of fusing to form the longer wormlike micelles.[70, 71] Transmission electron microscopy (TEM) was used in the current study to image the self-assembled morphologies giving rise to the differing dispersion properties observed and reported in the phase diagram above (Figure 1).
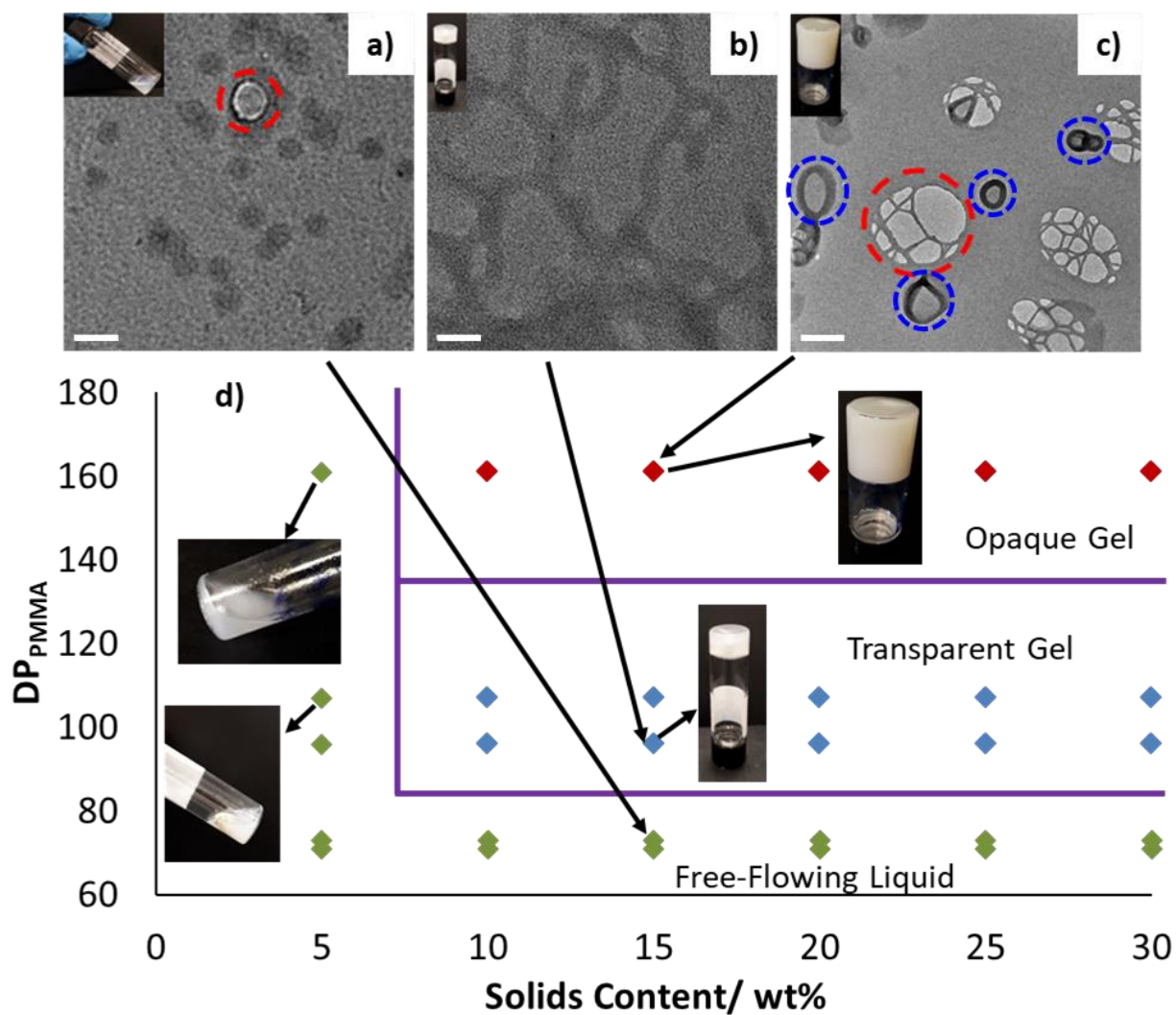
Figure 1. High resolution TEM images of the 3 different self-assembled structures dispersed at 15 wt% in *n*-decane; a: PI$_{32}$-*b*-PMMA$_{73}$ (scale bar = 50 nm), b: PI$_{32}$-*b*-PMMA$_{96}$ (scale bar = 50 nm), c: PI$_{32}$-*b*-PMMA$_{161}$ (scale bar = 200 nm) – vesicles indicated by blue dashed circles. d: Phase diagram generated for PI$_{32}$-*b*-PMMA$_{y}$ block copolymers, with varying degree of polymerisation, prepared by LAP-ATRP CHOMP, dispersed in *n*-decane. It should be noted that the features indicated with the red circle in 5a and 5c are part of the TEM grid and NOT a self-assembled nano-objects.

It can be challenging to image self-assembled block copolymers in which the core-forming block has a T_g below room temperature[26] although in some cases cryoTEM has been used to overcome these difficulties. In this study however, the core-forming PMMA block has a high T_g (105 ºC) whilst the corona-forming PI block has a T_g of −67 ºC. As such, the use of cryoTEM was not required, as has been shown to be the case in analogous studies of block copolymers with phenyl acrylate (T_g = 50 ºC) as the core-forming block.[72] TEM images of the different self-assembled morphologies of PI_{32}-b-$PMMA_y$ are shown in Figure 1. In each case the molar mass of the PI block remains constant with a DP of 32 and each image corresponds to a solids content of 15 wt%. Thus, the different morphologies arise purely as a function of the block length of the core-forming PMMA block. The sample with the lowest DP PMMA block (PI_{32}-b-$PMMA_{73}$) forms spherical micelles with uniform diameters of approximately 30 nm (Figure 1a), which accounts for the free-flowing liquid. This observation is consistent with expectations as a block copolymer comprising a lower mole fraction of the insoluble core-forming (PMMA) block would be expected to form spherical micelles in solution.[73] It should be noted that the feature indicated with the red circle is part of the grid and NOT a micelle. The TEM micrograph of PI_{32}-b-$PMMA_{96}$ (Figure 1b), with a larger core-forming block, clearly illustrates a different morphology and suggests that the self-supporting transparent gel is made up of wormlike micelles with diameters of a similar size to the spherical micelles formed from PI_{32}-b-$PMMA_{73}$. The TEM image (Figure 1c) of PI_{32}-b-$PMMA_{161}$, shows that the block copolymer with the largest PMMA block, formed vesicles (highlighted with blue dashed circles) which are up to 200 nm in diameter, approximately an order of magnitude larger than the size of the spherical micelles (in Figure 1a). The TEM images can be used to infer how the physical properties of each dispersion arise. The spherical micelles observed in Figure 1a are relatively small and therefore can flow past one another easily, hence forming a free-flowing

liquid. The phase diagram in Figure 1 shows that the same polymer sample remains mobile even at 30 wt%. The vesicles formed by PI$_{32}$-b-PMMA$_{161}$ at 15 wt% (Figure 1c) are also spherical but, being (at least) an order of magnitude larger than the spherical micelles, results in clustering, inhibiting their ability to flow at such a solids content. The impact of concentration has been discussed in the literature for the formation of free-flowing liquids by unentangled wormlike micelles at low concentrations (i.e. below the critical gelation concentration).[74] The wormlike micelles formed in the current study from PI$_{32}$-b-PMMA$_{96}$ at 15 wt% are dimensionally anisotropic with a length which is far greater than the cross-sectional diameter (estimated by TEM analysis). This results in significant entanglement and prevents the wormlike micelles from flowing on a short timescale, accounting for the formation of a self-supporting gel. These observations are consistent with reports in the literature.[26, 75] Analogous phase diagrams were also generated for the PI-b-PMMA BCPs prepared from PI$_{55}$-Br and PI$_{74}$-Br macroinitiators, dispersed in n-hexane and n-decane respectively (see Figure S6 in the supporting information). A direct comparison between the phase diagrams of PI$_{32}$-b-PMMA$_{x}$ and PI$_{74}$-b-PMMA$_{x}$ suggests that there is not a linear correlation between an increase in the molar mass of PI block and the increase in molar mass of PMMA required to achieve the equivalent phases in the phase diagram. This can be rationalised according to the Israelachvili packing parameter, as an increase in area per surface head group (i.e. MW$_{PI}$) causes a decrease in the packing parameter. This decrease can be offset to maintain the packing parameter by an increase in the volume of the core-forming block (i.e. MW$_{PMMA}$). However, this is not a scalar change because it will also cause an increased length of the core-forming block, decreasing the packing parameter further. To compensate for this, the volume must be increased further by an increase in the volume of the core-forming block (i.e. a greater proportional increase in MW$_{PMMA}$).

Having established (using TEM) the relationship between PMMA block length and/or concentration and morphology, dynamic light scattering (DLS) measurements were made on the free-flowing spherical micelles to ascertain particle size. DLS is a well-established technique for the characterisation of spherical particles, because the mathematics underpinning the calculation of particle size assumes all scattering events are from isotropic materials.[76] While it is also possible to use DLS for the characterisation of particles with anisotropic dimensions – e.g. worm-like micelles, it can be difficult to distinguish between sample anisotropy and size dispersity.[77] The DLS analysis of a dispersion of PI$_{32}$-b-PMMA$_{73}$ in n-decane (self-assembled at 15 wt%, but diuted to 0.72 wt% for DLS) is shown in Figure S7, which shows a single, monomodal peak with intensity-weighted average diameter of 62 nm (PDI = 0.117). This value is consistent with expectations in comparison to the TEM image for the same sample (Figure 1a) which showed spherical micelles with a diameter of approximately 25-30 nm. It is usual for DLS to indicate a larger particle size than TEM due to the differences in the measurement techniques. In particular, the hydrodynamic shell[78] and increased light scattering of larger particles has been shown to result in intensity-weighted particle size from DLS with larger values than seen by TEM.[79] The same phenomenon has also been observed for polymeric particles and micelles.[80, 81] Moreover, the DLS particle size distribution has a narrow dispersity which suggests that the combination of living anionic polymerisation and ATRP to prepare BCPs with a reasonably low dispersity in molar mass can be useful for preparing reasonably monodisperse self-assembled nanostructures.

Thermal Responsivity of Self-Assembled Morphologies

The response of self-assembled micellar structures to environmental stimuli such as temperature, salinity, pH etc. has been reported for micelles of both surfactants and block copolymers.[82] For example, cetyltrimethylammonium hydroxynaphthalene carboxylate (CTAHNC) is a surfactant

that forms vesicles at room temperature which undergo a vesicle to worm transition upon heating to 70 $^\circ$C, or a vesicle to worm transition upon the addition of cetyltrimethylammonium bromide (CTAB), a co-surfactant.[83] Similar phenomena have also been observed for micelles formed from diblock copolymers.[84-86] The rheological properties of self-assembled structures are of significant interest for many applications, providing information both on performance and processing properties.[87, 88] The impact of temperature on the rheological properties of such systems is inherently interesting and has been previously reported.[74, 89] In the current study, the self-supporting gels arising from wormlike micelles and vesicles are expected to exhibit more solid-like rheological properties, but may be expected to exhibit modified behaviour as the temperature is increased. A decreasing viscosity (with increasing temperature) can be very useful for mechanical processing, whilst an increasing viscosity can be useful for applications such as in viscosity modifiers.[90] Rheology curves illustrating the impact of temperature on the complex viscosity for the self-supporting gels formed by both wormlike micelles (a) and vesicles (b) are shown in Figure 2. The conditions for the temperature sweep (angular frequency = 1 rad s^{-1} and strain = 0.2) were derived from exploratory frequency sweeps for the samples which are shown in Figure S7.
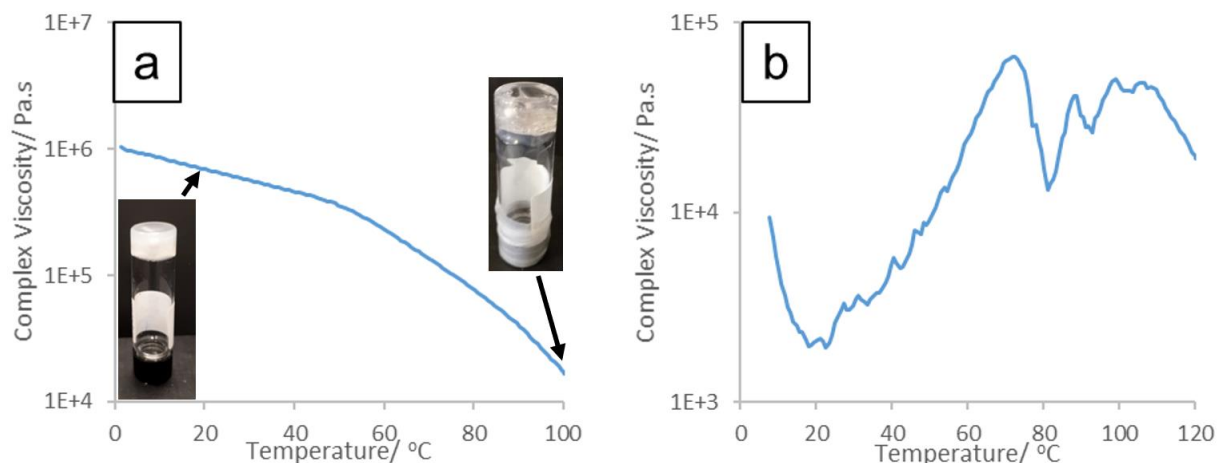
Figure 2. Logarithmic plot of complex viscosity versus temperature for 15 wt% dispersions in *n*-decane of a) PI_{32}-*b*-$PMMA_{96}$, and b) PI_{32}-*b*-$PMMA_{161}$. Inset photographs in a) of sample dispersions at temperatures indicated on graph. Complex viscosity calculation described in experimental

A plot of the log complex viscosity versus temperature for PI_{32}-*b*-$PMMA_{96}$ (Figure 2a), which at 15 wt% forms a self-supporting gel of worm-like micelles at room temperature, shows an almost linear, but shallow, decrease in log complex viscosity from 0 - 50 °C, at which temperature the plot shows an abrupt change in gradient. The likely explanation for this phenomenon is a slight increase in solvation of the core-forming PMMA block in *n*-decane at higher temperature, which results in interfacial plasticisation of the core of the micelles (i.e. the PMMA closest to the polyisoprene block). The phenomenon of interfacial plasticisation arising due to partial solvation of the core-forming block in BCP micelles has been previously reported.[84, 91-93] This enhanced solvation can cause the ratio of soluble polymer: insoluble polymer, in the BCP to increase, with a concomitant increase in curvature of micelles. The abrupt change in the gradient of log complex viscosity versus temperature for PI_{32}-*b*-$PMMA_{96}$ at 50 °C is difficult to rationalise with certainty without *in situ* TEM characterisation. However, the inset photographs of the sample in Figure 2a

show that the sample becomes far more transparent at higher temperatures and begins to show some signs of flow, which would suggest the onset of a change in morphology. Similar observations have previously been reported by Fielding *et al.* for the reversible gelation of a poly(lauryl methacrylate)$_{16}$-*block*-poly(benzyl methacrylate)$_{37}$ copolymer.[84] Upon heating above 50 °C, de-gelation occurred because of a partial transition from wormlike to spherical micelles which reduces the entanglement of the remaining worms in solution. Ratcliffe *et al.* reported similar behaviour[26] for a poly(lauryl acrylate)–poly(benzyl acrylate) block copolymer which was reportedly a stiff gel at 4 °C that became softer at 20 °C and finally a free-flowing liquid at 80 °C. This behaviour was explained by a change in properties of the core-forming PBzA block with a T_g of 6 °C and "debranching", leaving "free" disentangled worms in solution that form a softer gel before a full transition to spherical micelles. The results in the current study for PI$_{32}$-*b*-PMMA$_{96}$ (Figure 2a) would suggest that the latter (debranching) explanation is more plausible given that the T_g of the core-forming PMMA block (105 °C) in the current work is far higher than the transition point observed in the rheology (50 °C). It is unlikely that a full morphological transition from wormlike to spherical micelles has taken place at 100 °C because the storage and loss moduli have not crossed over (see Figure S9) and the complex viscosity remains several orders of magnitude higher than that of the PI$_{32}$-*b*-PMMA$_{73}$ sample which self-assembled into spherical micelles at 15 wt% in *n*-decane (see Figure S10). The evidence therefore points towards the onset of a transition at 50 °C from entangled wormlike micelles to shorter, disentangled worms accompanied by a pronounced decline in the viscosity. It is likely that the sample exists as a mixture of wormlike micelles, some of which remain entangled in a 3D network, and also a small proportion of spherical micelles at 100 °C. This is also consistent with a convergence of the storage and loss moduli in the rheology plot which is shown in Figure S9. It is most likely that if the

temperature was increased further, a steeper decline in the complex viscosity would result as the free worms complete the transition to spherical micelles.

At ambient temperature a 15 wt% dispersion of PI_{32}-b-$PMMA_{161}$ in n-decane forms vesicles. The plot of log complex viscosity against temperature is shown in Figure 2b. At 10 °C the complex viscosity of PI_{32}-b-$PMMA_{161}$ is about 2 orders of magnitude lower than that seen for PI_{32}-b-$PMMA_{96}$ (Figure 2a), which exists as wormlike micelles at the same temperature. The lower viscosity of dispersions of vesicles, compared to worms, has been particularly well-demonstrated recently by Ratcliffe et $al.$ for a single sample of (thermoresponsive) block copolymer that can form spheres, worms and vesicles at different temperatures.[94] Ratcliffe reported rheological analysis showing a maximum in the complex viscosity at 14 °C, arising due to the formation of wormlike micelles, with a complex viscosity which is approximately 2 orders of magnitude greater than that of spherical micelles (formed upon cooling) and vesicles (formed upon heating). In the current work, Figure 2b illustrates that as the temperature was increased from 20 to 70 °C the complex viscosity of PI_{32}-b-$PMMA_{161}$ rises by almost 2 orders of magnitude, which could reasonably be assumed to arise due to a transition in morphology from vesicles to wormlike micelles, as the PMMA undergoes interfacial plasticization and an increase in the area of the corona-forming head group. Similar observations of a higher viscosity with increasing temperature were reported by Derry et $al.$ for self-assembled PSMA-b-PBzMA BCPs dispersed in a non-polar base oil.[90] In that case, TEM characterisation of samples before and after heating, and variable temperature SAXS, were used to illustrate the transition in morphology. The authors concluded that the transition was due to increased solvation of the insoluble PBzMA core-forming block. Above 70 °C, the complex viscosity data for PI_{32}-b-$PMMA_{161}$ (Figure 2b) becomes erratic however, one might tentatively suggest that the apparent maximum in viscosity at 70 °C, followed

by a (noisy) decrease in complex viscosity above that temperature, is due to the onset of transition of the wormlike micelles towards spherical micelles.

For completeness, the analogous rheology curve for the dispersion in n-decane of 15 wt% of PI$_{32}$-b-PMMA$_{73}$, which formed a free-flowing liquid dispersion of spherical micelles, is shown in supporting information as Figure S10. In this case the complex viscosity was constant at 0.020 Pa.s across the entire temperature range from 25 – 115 °C and very much lower than the complex viscosity of both samples illustrated in Figure 2, which is to be expected for a free-flowing liquid.

With the aim of providing further evidence to support the hypothesis that an increase in temperature drives a change in self-assembled morphology, TEM was used to image a dispersion of PI$_{32}$-b-PMMA$_{96}$ (15 wt% in n-decane), that exists as wormlike micelles at room temperature (see Figure 1), after heating to 150 °C for 10 minutes, which is well above the temperature at which a change in the complex viscosity was observed (Figure 2a). The expectation is that at this elevated temperature the morphology should switch from worms to spherical micelles. The heated sample was then diluted to 1 wt% in n-decane, at the elevated temperature. Whilst the formation of wormlike micelles is thermodynamically favoured (for this sample) at room temperature, and one might expect any heat-induced transition in morphology to be reversed upon cooling, drastic dilution of the dispersion after any potential transition in morphology to spherical micelles decreases the probability of the spherical micelles colliding in order to re-fuse into wormlike micelles. In effect, dilution kinetically traps any newly-formed morphology upon heating, and is in keeping with previous reports of imaging of thermally-induced morphology transitions.[84, 90, 95] The diluted dispersion was allowed to cool to room temperature. A control sample was also prepared by diluting (without heating) the same sample from 15 wt% to 1 wt% at room temperature. TEM images of the 2 samples are shown below in Figure 3.
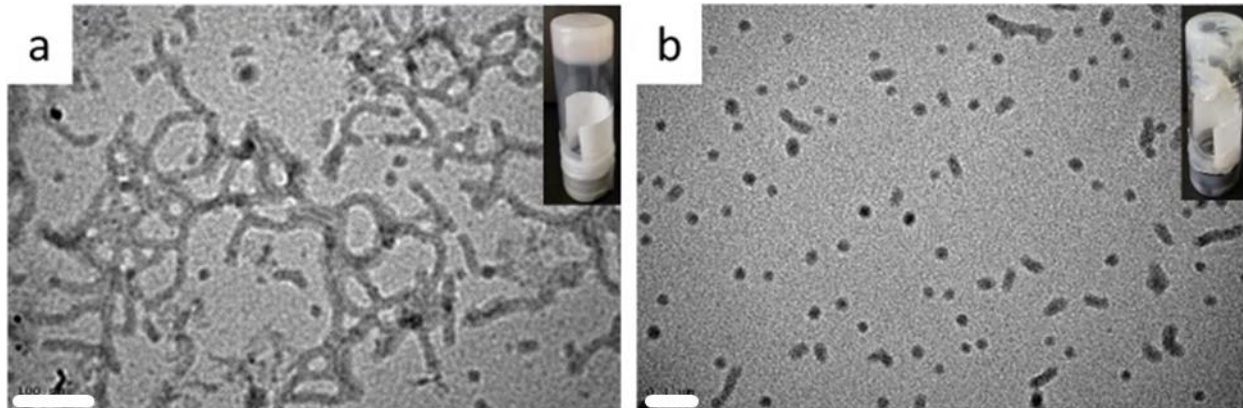
Figure 3. High resolution TEM images of PI_{32}-b-$PMMA_{96}$, dispersed at 15 wt% in n-decane at room temperature before a) dilution with n-decane to 1 wt% at room temperature and b) dilution to 1 wt% at 150 °C by the addition of n-decane, followed by cooling to room temperature. Scale bar = 100 nm.

The TEM image of PI_{32}-b-$PMMA_{96}$ which was diluted to 1 wt% at room temperature (Figure 3a) shows a mixed morphology which is dominated by wormlike micelles, and displays a very similar morphology to the same sample 15 wt%, prior to dilution (see Figure 1). This clearly illustrates that the wormlike morphology is conserved upon dilution at room temperature, confirming that dilution alone does not lead to a change in morphology. The TEM image in Figure 3b shows PI_{32}-b-$PMMA_{96}$ after heating to 150 °C <u>before</u> dilution to 1 wt% (at 150 °C) followed by cooling to allow characterisation, clearly shows a morphology of predominantly spherical micelles and a few short wormlike micelles (c. 100 nm in length). Having established that the initial worm-like morphology is unaffected by dilution alone, this image suggests a change in morphology from worms to spheres occurs upon heating, with the second morphology being trapped by dilution to 1 wt%. The change in morphology at high temperature is consistent with the observed decrease in complex viscosity shown in Figure 2a. The most plausible explanation for a

transition in morphology, as suggested above, is partial solvation of the core-forming PMMA in *n*-decane. A thermally-induced transition from worm-like to spherical micelles of PDMAEMA-*b*-PPMA BCPs dispersed in ethanol has previously been described by Pei *et al.*, who used TEM characterisation coupled with 'hot dilution' to trap the newly formed spherical morphology.[96] Pei also used variable temperature proton NMR and showed that the peaks for the core-forming PPMA block increased in intensity at high temperature, suggesting increased solvation of the core-forming block in agreement with the hypothesis proposed above.

The effect of hysteresis upon heating/cooling was also investigated by heating a 15 wt% dispersion in *n*-decane of PI$_{32}$-*b*-PMMA$_{96}$ and then cooling without dilution. Thus, the sample which self-assembles into wormlike micelles at room temperature was heated to 150 $^{\circ}$C, the temperature previously shown to induce a change in morphology to spherical micelles (Figure 3), held for 15 minutes in a sealed system to prevent any loss of solvent, before cooling to room temperature. TEM images of the cooled sample gel (Figure S11) showed a morphology consisting of worm-like micelles of diameter approximately 20 nm, which is practically identical to the TEM image (Figure 1) of the sample prior to being heated. This, would appear to confirm that the worm-like micelles of PI$_{32}$-*b*-PMMA$_{96}$ in *n*-decane transition to spherical micelles upon heating to 150 $^{\circ}$C, which, if not trapped by dilution, revert back to the thermodynamically-favoured worm-like morphology upon cooling to room temperature. In this respect the behavior of the PI-*b*-PMMA block copolymers is analogous to that previously reported by Blanazs *et al* for thermoresponsive PGMA-*b*-PHPMA diblock copolymers, dispersed in water.[97]

CONCLUSION

A family of polyisoprene-*block*-poly(methyl methacrylate) block copolymers have been prepared by a change of mechanism polymerisation in which an ATRP polyisoprene macroinitiator

was synthesised by living anionic polymerisation. The use of living anionic polymerisation enables the scalable and quantitative polymerisation of isoprene with well-controlled molar mass and a narrow dispersity. Moreover by fixing the molar mass of the polyisoprene block length, and varying the molar mass of PMMA, three homologous series of block copolymers were prepared and fully characterised using proton NMR spectroscopy. The resulting block copolymers were dispersed in n-decane (or n-hexane), a selective solvent for the polyisoprene block, at high solids contents of up to 30 wt% to investigate block copolymer self-assembly.

By varying the molecular weight of the core-forming PMMA block, a variety of morphologies could be generated. These were characterised by DLS and TEM and shown to be spherical micelles, wormlike micelles and vesicles. Thermoresponsivity has been demonstrated in so much that it is possible to transition between different self-assembled morphologies by varying the temperature. In particular it has been shown for a 15 wt% dispersion in n-decane of PI_{32}-b-$PMMA_{96}$ an increase in temperature results in the onset of a transition from worm-like to spherical micelles, as evidenced by an abrupt change in complex viscosity above 50 $^{\circ}$C and TEM analysis of the newly formed spherical micelles, trapped by dilution at 150 $^{\circ}$C. The conclusion that a transition in morphology arises due to enhanced solvation of the core-forming block, and a change in the Israelachvili packing parameter, is supported by the literature. Control experiments unambiguously show that the transition is not triggered by dilution alone and that cooling without dilution causes the spherical micelles to revert to initial worm-like morphology – thereby also demonstrating thermoreversibility. Furthermore, complex viscosity data suggests analogous behavior for PI_{32}-b-$PMMA_{161}$ which transitions from (lower viscosity) vesicles at room temperature to (higher viscosity) worm-like micelles at 70 degrees.

Although the current study focusses on the synthesis and characterisation of PI-*b*-PMMA block copolymers, the use of living anionic polymerisation in combination with ATRP offers an extraordinarily versatile and scalable approach for the preparation of block copolymers, with almost infinite variability in terms of molar mass and composition. One might expect similar versatility in terms of physical (thermoresponsive) properties following self-assembly in selective solvents.

SUPPORTING INFORMATION

Supporting information related to the molecular analysis of the block copolymers (SEC and NMR), their self-assembled morphologies (TEM) and complex rheology is supplied as Table S2 and Figures S1 – S11.

ACKNOWLEDGEMENTS

REFERENCES

(1) Climie, I. E.; White, E. F. T. The Aggregation of Random and Block Copolymers Containing Acrylonitrile in Mixed Solvents. *J. Polym. Sci.* **1960**, *47*, 149-156.

(2) Krause, S. Dilute Solution Properties of Styrene-Methyl Methacrylate Block Copolymer. *J. Phys. Chem.* **1964**, *68*, 1948-1955.

(3) Szwarc, M. 'Living' Polymers. *Nature* **1956**, *178*, 1168-1169.

(4) Bahadur, P.; Sastry, N. V.; Marti, S.; Riess, G. Micellar Behavior of Styrene Isoprene Block Copolymers in Selective Solvents. *Colloids Surf.* **1985**, *16*, 337-346.

(5) Hodrokoukes, P.; Pispas, S.; Hadjichristidis, N. Controlling micellar properties of styrene/isoprene copolymers by altering the monomer arrangement along the chain. *Macromolecules* **2002**, *35*, 834-840.

(6) Baskaran, D. Strategic developments in living anionic polymerization of alkyl (meth)acrylates. *Prog. Polym. Sci.* **2003**, *28*, 521-581.

(7) Szwarc, M.; Rembaum, A. Polymerization of Methyl Methacrylate Initiated by an Electron Transfer to the Monomer. *J. Polym. Sci.* **1956**, *22*, 189-191.

(8) Kunkel, D.; Muller, A. H. E.; Janata, M.; Lochmann, L. The Role of Association/Complexation Equilibria in the Anionic-Polymerization of (Meth)acrylates. *Makromol. Chem., Macromol. Symp.* **1992**, *60*, 315-326.

(9) Vlcek, P.; Lochmann, L. Anionic polymerization of (meth)acrylate esters in the presence of stabilizers of active centres. *Prog. Polym. Sci.* **1999**, *24*, 793-873.

(10) Vlcek, P.; Cadova, E.; Horsky, J.; Janata, M. MALDI-TOF MS analysis of the self-termination products in the anionic methyl methacrylate/tert-butyl acrylate block copolymerization. *Polym. Bull.* **2015**, *72*, 2227-2239.

(11) Goode, W. E.; Snyder, W. H.; Fettes, R. C. Anionic Polymerization - Mechanism of Methyl Methacrylate Polymerizations Initiated by Metal Amides in Liquid Ammonia. *J. Polym. Sci.* **1960**, *42*, 367-382.

(12) Baskaran, D.; Chakrapani, S.; Sivaram, S. Effect of Chelation of the Lithium Cation on the Anionic-Polymerization of Methyl-Methacrylate Using Organolithium Initiators. *Macromolecules* **1995**, *28*, 7315-7317.

(13) Jacobs, C.; Varshney, S. K.; Hautekeer, J. P.; Fayt, R.; Jerome, R.; Teyssie, P. Termination Mechanism in the Anionic Copolymerization of Methyl-Methacrylate and Tert-Butyl Acrylate. *Macromolecules* **1990**, *23*, 4024-4025.

(14) Fayt, R.; Forte, R.; Jacobs, C.; Jerome, R.; Ouhadi, T.; Teyssie, P.; Varshney, S. K. New Initiator System for the Living Anionic-Polymerization of Tert-Alkyl Acrylates. *Macromolecules* **1987**, *20*, 1442-1444.

(15) Wang, J. S.; Matyjaszewski, K. Controlled Living Radical Polymerization - Atom-Transfer Radical Polymerization in the Presence of Transition-Metal Complexes. *J. Am. Chem. Soc.* **1995**, *117*, 5614-5615.

(16) Kato, M.; Kamigaito, M.; Sawamoto, M.; Higashimura, T. Polymerization of Methyl-Methacrylate with the Carbon-Tetrachloride Dichlorotris(Triphenylphosphine)Ruthenium(II) Methylaluminum Bis(2,6-Di-Tert-Butylphenoxide) Initiating System - Possibility of Living Radical Polymerization. *Macromolecules* **1995**, *28*, 1721-1723.

(17) Chiefari, J.; Chong, Y. K.; Ercole, F.; Krstina, J.; Jeffery, J.; Le, T. P. T.; Mayadunne, R. T. A.; Meijs, G. F.; Moad, C. L.; Moad, G.; Rizzardo, E.; Thang, S. H. Living free-radical

polymerization by reversible addition-fragmentation chain transfer: The RAFT process. *Macromolecules* **1998**, *31*, 5559-5562.

(18) Karagoz, B.; Esser, L.; Duong, H. T.; Basuki, J. S.; Boyer, C.; Davis, T. P. Polymerization-Induced Self-Assembly (PISA) - control over the morphology of nanoparticles for drug delivery applications. *Polym. Chem.* **2014**, *5*, 350-355.

(19) Nunes, S. P. Block Copolymer Membranes for Aqueous Solution Applications. *Macromolecules* **2016**, *49*, 2905-2916.

(20) Segalman, R. A. Patterning with block copolymer thin films. *Mater. Sci. Eng. R Rep.* **2005**, *48*, 191-226.

(21) Fielding, L. A.; Derry, M. J.; Ladmiral, V.; Rosselgong, J.; Rodrigues, A. M.; Ratcliffe, L. P. D.; Sugihara, S.; Armes, S. P. RAFT dispersion polymerization in non-polar solvents: facile production of block copolymer spheres, worms and vesicles in n-alkanes. *Chem. Sci.* **2013**, *4*, 2081-2087.

(22) Schmidt, B. Double Hydrophilic Block Copolymer Self-Assembly in Aqueous Solution. *Macromol. Chem. Phys.* **2018**, *219*, 1700494.

(23) Giacomelli, C.; Schmidt, V.; Borsali, R. Nanocontainers formed by self-assembly of poly(ethylene oxide)-b-poly(glycerol monomethacrylate) - Drug conjugates. *Macromolecules* **2007**, *40*, 2148-2157.

(24) Li, C. H.; Ge, Z. S.; Fang, J.; Liu, S. Y. Synthesis and Self-Assembly of Coil-Rod Double Hydrophilic Diblock Copolymer with Dually Responsive Asymmetric Centipede-Shaped Polymer Brush as the Rod Segment. *Macromolecules* **2009**, *42*, 2916-2924.

(25) Alexandridis, P.; Hatton, T. A. Poly(Ethylene Oxide)-Poly(Propylene Oxide)-Poly(Ethylene Oxide) Block-Copolymer Surfactants in Aqueous-Solutions and at Interfaces - Thermodynamics, Structure, Dynamics, and Modelling. *Colloids Surf. A Physicochem. Eng. Asp.* **1995**, *96*, 1-46.

(26) Ratcliffe, L. P. D.; McKenzie, B. E.; Le Bouëdec, G. M. D.; Williams, C. N.; Brown, S. L.; Armes, S. P. Polymerization-Induced Self-Assembly of All-Acrylic Diblock Copolymers via RAFT Dispersion Polymerization in Alkanes. *Macromolecules* **2015**, *48*, 8594-8607.

(27) Growney, D. J.; Mykhaylyk, O. O.; Armes, S. P. Micellization and adsorption behavior of a near-monodisperse polystyrene-based diblock copolymer in nonpolar media. *Langmuir* **2014**, *30*, 6047-56.

(28) Derry, M. J.; Fielding, L. A.; Armes, S. P. Industrially-relevant polymerization-induced self-assembly formulations in non-polar solvents: RAFT dispersion polymerization of benzyl methacrylate. *Polym. Chem.* **2015**, *6*, 3054-3062.

(29) Derry, M. J.; Fielding, L. A.; Armes, S. P. Polymerization-induced self-assembly of block copolymer nanoparticles via RAFT non-aqueous dispersion polymerization. *Prog. Polym. Sci.* **2016**, *52*, 1-18.

(30) Mable, C. J.; Warren, N. J.; Thompson, K. L.; Mykhaylyk, O. O.; Armes, S. P. Framboidal ABC triblock copolymer vesicles: a new class of efficient Pickering emulsifier. *Chem Sci* **2015**, *6*, 6179-6188.

(31) Obeng, M.; Milani, A. H.; Musa, M. S.; Cui, Z. X.; Fielding, L. A.; Farrand, L.; Goulding, M.; Saunders, B. R. Self-assembly of poly(lauryl methacrylate)-b-poly(benzyl methacrylate) nano-objects synthesised by ATRP and their temperature-responsive dispersion properties. *Soft Matter* **2017**, *13*, 2228-2238.

(32) Zhang, L. F.; Eisenberg, A. Multiple morphologies and characteristics of "crew-cut" micelle-like aggregates of polystyrene-b-poly(acrylic acid) diblock copolymers in aqueous solutions. *J. Am. Chem. Soc.* **1996**, *118*, 3168-3181.

(33) Zhang, L. F.; Eisenberg, A. Formation of crew-cut aggregates of various morphologies from amphiphilic block copolymers in solution. *Polym. Adv. Technol.* **1998**, *9*, 677-699.

(34) Jitchum, V.; Perrier, S. Living radical polymerization of isoprene via the RAFT process. *Macromolecules* **2007**, *40*, 1408-1412.

(35) Wootthikanokkhan, J.; Peesan, M.; Phinyocheep, P. Atom transfer radical polymerizations of (meth)acrylic monomers and isoprene. *Eur. Polym. J.* **2001**, *37*, 2063-2071.

(36) Acar, M. H.; Matyjaszewski, K. Block copolymers by transformation of living anionic polymerization into controlled/"living' atom transfer radical polymerization. *Macromol. Chem. Phys.* **1999**, *200*, 1094-1100.

(37) Hillmyer, M. Block copolymer synthesis. *Curr. Opin. Solid State Mater. Sci.* **1999**, *4*, 559-564.

(38) Castle, T. C.; Khosravi, E.; Hutchings, L. R. Block copolymers by the conversion of living lithium initiated anionic polymerization into living ruthenium ROMP. *Macromolecules* **2006**, *39*, 5639-5645.

(39) Katayama, H.; Yonezawa, F.; Nagao, M.; Ozawa, F. Ring-opening metathesis polymerization of norbornene using vinylic ethers as chain-transfer agents: Highly selective synthesis of monofunctional macroinitiators for atom transfer radical polymerization. *Macromolecules* **2002**, *35*, 1133-1136.

(40) Lee, D. C.; Lamm, R. J.; Prossnitz, A. N.; Boydston, A. J.; Pun, S. H. Dual Polymerizations: Untapped Potential for Biomaterials. *Adv. Healthc. Mater.* **2019**, *8*, 1800861.

(41) Castle, T. C.; Hutchings, L. R.; Khosravi, E. Synthesis of block copolymers by changing living anionic polymerization into living ring opening metathesis polymerization. *Macromolecules* **2004**, *37*, 2035-2040.

(42) Benoit, D.; Harth, E.; Fox, P.; Waymouth, R. M.; Hawker, C. J. Accurate Structural Control and Block Formation in the Living Polymerization of 1,3-Dienes by Nitroxide-Mediated Procedures. *Macromolecules* **2000**, *33*, 363-370.

(43) Jitchum, V.; Perrier, S. Living Radical Polymerization of Isoprene via the RAFT Process. *Macromolecules* **2007**, *40*, 1408-1412.

(44) Bar-Nes, G.; Hall, R.; Sharma, V.; Gaborieau, M.; Lucas, D.; Castignolles, P.; Gilbert, R. G. Controlled/living radical polymerization of isoprene and butadiene in emulsion. *Eur. Polym. J.* **2009**, *45*, 3149-3163.

(45) Zhu, Y. F.; Jiang, F. J.; Zhang, P. P.; Luo, J.; Tang, H. D. Atom transfer radical polymerization and copolymerization of isoprene catalyzed by copper bromide/2,2′-bipyridine. *Chin. Chem. Lett.* **2016**, *27*, 910-914.

(46) Fischer, H. The persistent radical effect in "living" radical polymerization. *Macromolecules* **1997**, *30*, 5666-5672.

(47) Fischer, H. The persistent radical effect in controlled radical polymerizations. *J. Polym. Sci. Pol. Chem.* **1999**, *37*, 1885-1901.

(48) Zhu, Y. F.; Jiang, F. J.; Zhang, P. P.; Luo, J.; Tang, H. D. Atom transfer radical polymerization and copolymerization of isoprene catalyzed by copper bromide/2,2 '-bipyridine. *Chin. Chem. Lett.* **2016**, *27*, 910-914.

(49) Vasu, V.; Kim, J. S.; Yu, H. S.; Bannerman, W. I.; Johnson, M. E.; Asandei, A. D. Toward Butadiene-ATRP with Group 10 (Ni, Pd, Pt) Metal Complexes. *ACS Symp. Ser.* **2018**, *1284*, 205-225.

(50) Darmau, B.; Rymaruk, M. J.; Warren, N. J.; Bening, R.; Armes, S. P. RAFT dispersion polymerization of benzyl methacrylate in non-polar media using hydrogenated polybutadiene as a steric stabilizer block. *Polymer Chemistry* **2020**.

(51) O'Reilly, R. K.; Hawker, C. J.; Wooley, K. L. Cross-linked block copolymer micelles: functional nanostructures of great potential and versatility. *Chem. Soc. Rev.* **2006**, *35*, 1068-83.

(52) Valkama, S.; Ruotsalainen, T.; Nykänen, A.; Laiho, A.; Kosonen, H.; Brinke, G. t.; Ikkala, O.; Ruokolainen, J. Self-Assembled Structures in Diblock Copolymers with Hydrogen-Bonded Amphiphilic Plasticizing Compounds. *Macromolecules* **2006**, *39*, 9327-9336.

(53) Bowers, J.; Zarbakhsh, A.; Webster, J. R. P.; Hutchings, L. R.; Richards, R. W. Structure of a Spread Film of a Polybutadiene-Poly(ethylene oxide) Linear Diblock Copolymer at the Air-Water Interface As Determined by Neutron Reflectometry. *Langmuir* **2001**, *17*, 131-139.

(54) Herzberger, J.; Niederer, K.; Pohlit, H.; Seiwert, J.; Worm, M.; Wurm, F. R.; Frey, H. Polymerization of Ethylene Oxide, Propylene Oxide, and Other Alkylene Oxides: Synthesis, Novel Polymer Architectures, and Bioconjugation. *Chem Rev* **2016**, *116*, 2170-243.

(55) Quirk, R. P.; Ma, J. J. Characterization of the Functionalization Reaction-Product of Poly(Styryl)Lithium with Ethylene-Oxide. *J. Polym. Sci. Pol. Chem.* **1988**, *26*, 2031-2037.

(56) Liu, B.; Liu, F.; Luo, N.; Ying, S. K.; Liu, Q. Synthesis of block copolymer by integrated living anionic polymerization-atom transfer radical polymerization (ATRP). *Chin. J. Polym. Sci.* **2000**, *18*, 39-43.

(57) Wang, G.; Schmitt, M.; Wang, Z.; Lee, B.; Pan, X.; Fu, L.; Yan, J.; Li, S.; Xie, G.; Bockstaller, M. R.; Matyjaszewski, K. Polymerization-Induced Self-Assembly (PISA) Using ICAR ATRP at Low Catalyst Concentration. *Macromolecules* **2016**, *49*, 8605-8615.

(58) Zhu, G.; Zhang, L.; Zhang, Z.; Zhu, J.; Tu, Y.; Cheng, Z.; Zhu, X. Iron-Mediated ICAR ATRP of Methyl Methacrylate. *Macromolecules* **2011**, *44*, 3233-3239.

(59) Kwak, Y.; Matyjaszewski, K. ARGET ATRP of methyl methacrylate in the presence of nitrogen-based ligands as reducing agents. *Polym. Int.* **2009**, *58*, 242-247.

(60) Queffelec, J.; Gaynor, S. G.; Matyjaszewski, K. Optimization of Atom Transfer Radical Polymerization Using Cu(I)/ Tris(2-(dimethylamino)ethyl)amine as a Catalyst. *Macromolecules* **2000**, *33*, 8629-8639.

(61) Matyjaszewski, K.; Shipp, D. A.; Wang, J.-L.; Grimaud, T.; Patten, T. E. Utilizing Halide Exchange To Improve Control of Atom Transfer Radical Polymerization. *Macromolecules* **1998**, *31*, 6836-6840.

(62) Wang, J. L.; Grimaud, T.; Matyjaszewski, K. Kinetic Study of the Homogeneous Atom Transfer Radical Polymerization of Methyl Methacrylate. *Macromolecules* **1997**, *30*, 6507-6512.

(63) Tanaka, H.; Yamauchi, K.; Hasegawa, H.; Miyamoto, N.; Koizumi, S.; Hashimoto, T. In situ and real-time small-angle neutron scattering studies of living anionic polymerization process and polymerization-induced self-assembly of block copolymers. *Physica B Condens. Matter.* **2006**, *385*, 742-744.

(64) Wu, J.; Tian, C.; Zhang, L.; Cheng, Z.; Zhu, X. Synthesis of soap-free emulsion with high solid content by differential dripping RAFT polymerization-induced self-assembly. *RSC Adv.* **2017**, *7*, 6559-6564.

(65) Canning, S. L.; Smith, G. N.; Armes, S. P. A Critical Appraisal of RAFT-Mediated Polymerization-Induced Self-Assembly. *Macromolecules* **2016**, *49*, 1985-2001.

(66) Mai, Y.; Eisenberg, A. Self-assembly of block copolymers. *Chem. Soc. Rev.* **2012**, *41*, 5969-85.

(67) Atanase, L. I.; Riess, G. Self-Assembly of Block and Graft Copolymers in Organic Solvents: An Overview of Recent Advances. *Polymers* **2018**, *10*, 26.

(68) Blanazs, A.; Ryan, A. J.; Armes, S. P. Predictive Phase Diagrams for RAFT Aqueous Dispersion Polymerization: Effect of Block Copolymer Composition, Molecular Weight, and Copolymer Concentration. *Macromolecules* **2012**, *45*, 5099-5107.

(69) Yang, P. C.; Ratcliffe, L. P. D.; Armes, S. P. Efficient Synthesis of Poly(methacrylic acid)-block-Poly(styrene-alt-N-phenylmaleimide) Diblock Copolymer Lamellae Using RAFT Dispersion Polymerization. *Macromolecules* **2013**, *46*, 8545-8556.

(70) Blanazs, A.; Madsen, J.; Battaglia, G.; Ryan, A. J.; Armes, S. P. Mechanistic Insights for Block Copolymer Morphologies: How Do Worms Form Vesicles? *J. Am. Chem. Soc.* **2011**, *133*, 16581-16587.

(71) Warren, N. J.; Mykhaylyk, O. O.; Mahmood, D.; Ryan, A. J.; Armes, S. P. RAFT Aqueous Dispersion Polymerization Yields Poly(ethylene glycol)-Based Diblock Copolymer Nano-Objects with Predictable Single Phase Morphologies. *J. Am. Chem. Soc.* **2014**, *136*, 1023-1033.

(72) Canning, S. L.; Cunningham, V. J.; Ratcliffe, L. P. D.; Armes, S. P. Phenyl acrylate is a versatile monomer for the synthesis of acrylic diblock copolymer nano-objects via polymerization-induced self-assembly. *Polym. Chem.* **2017**, *8*, 4811-4821.

(73) Israelachvili, J. N.; Mitchell, D. J.; Ninham, B. W. Theory of Self-Assembly of Hydrocarbon Amphiphiles into Micelles and Bilayers. *J. Chem. Soc., Faraday Trans. 2* **1976**, *72*, 1525-1568

(74) Lovett, J. R.; Derry, M. J.; Yang, P. C.; Hatton, F. L.; Warren, N. J.; Fowler, P. W.; Armes, S. P. Can percolation theory explain the gelation behavior of diblock copolymer worms? *Chem. Sci.* **2018**, *9*, 7138-7144.

(75) Ladmiral, V.; Charlot, A.; Semsarilar, M.; Armes, S. P. Synthesis and characterization of poly(amino acid methacrylate)-stabilized diblock copolymer nano-objects. *Polym. Chem.* **2015**, *6*, 1805-1816.

(76) Gohy, J. F.; Varshney, S. K.; Jérôme, R. Water-Soluble Complexes Formed by Poly(2-vinylpyridinium)-block-poly(ethylene oxide) and Poly(sodium methacrylate)-block-poly(ethylene oxide) Copolymers. *Macromolecules* **2001**, *34*, 3361-3366.

(77) Guérin, G.; Raez, J.; Manners, I.; Winnik, M. A. Light Scattering Study of Rigid, Rodlike Organometallic Block Copolymer Micelles in Dilute Solution. *Macromolecules* **2005**, *38*, 7819-7827.

(78) Pabisch, S.; Feichtenschlager, B.; Kickelbick, G.; Peterlik, H. Effect of interparticle interactions on size determination of zirconia and silica based systems - A comparison of SAXS, DLS, BET, XRD and TEM. *Chem. Phys. Lett.* **2012**, *521*, 91-97.

(79) Souza, T. G. F.; Ciminelli, V. S. T.; Mohallem, N. D. S. A comparison of TEM and DLS methods to characterize size distribution of ceramic nanoparticles. *J. Phys. Conf. Ser.* **2016**, *733*.

(80) Bootz, A.; Vogel, V.; Schubert, D.; Kreuter, J. Comparison of scanning electron microscopy, dynamic light scattering and analytical ultracentrifugation for the sizing of poly(butyl cyanoacrylate) nanoparticles. *Eur. J. Pharm. Biopharm.* **2004**, *57*, 369-375.

(81) Xu, Q. H.; Tian, C.; Zhang, L. F.; Cheng, Z. P.; Zhu, X. L. Photo-Controlled Polymerization-Induced Self-Assembly (Photo-PISA): A Novel Strategy Using In Situ Bromine-Iodine Transformation Living Radical Polymerization. *Macromol. Rapid Commun.* **2019**, *40*, 6.

(82) Feng, Y.; Chu, Z.; Dreiss, C. A., *Smart Wormlike Micelles*. 2015; Vol. 42, p 7174-7203.

(83) Hassan, P. A.; Valaulikar, B. S.; Manohar, C.; Kern, F.; Bourdieu, L.; Candau, S. J. Vesicle to micelle transition: Rheological investigations. *Langmuir* **1996**, *12*, 4350-4357.

(84) Fielding, L. A.; Lane, J. A.; Derry, M. J.; Mykhaylyk, O. O.; Armes, S. P. Thermo-responsive Diblock Copolymer Worm Gels in Non-polar Solvents. *J. Am. Chem. Soc.* **2014**, *136*, 5790-5798.

(85) Warren, N. J.; Mykhaylyk, O. O.; Mahmood, D.; Ryan, A. J.; Armes, S. P. RAFT aqueous dispersion polymerization yields poly(ethylene glycol)-based diblock copolymer nano-objects with predictable single phase morphologies. *J. Am. Chem. Soc.* **2014**, *136*, 1023-33.

(86) Canning, S. L.; Neal, T. J.; Armes, S. P. pH-Responsive Schizophrenic Diblock Copolymers Prepared by Polymerization-Induced Self-Assembly. *Macromolecules* **2017**, *50*, 6108-6116.

(87) Seitz, M. E.; Burghardt, W. R.; Faber, K. T.; Shull, K. R. Self-Assembly and Stress Relaxation in Acrylic Triblock Copolymer Gels. *Macromolecules* **2007**, *40*, 1218-1226.

(88) Bhatia, S. R.; Mourchida, A.; Joanicot, M. Block copolymer assembly to control fluid rheology. *Curr. Opin. Colloid Interface Sci* **2001**, *6*, 471-478.

(89) Lopez-Oliva, A. P.; Warren, N. J.; Rajkumar, A.; Mykhaylyk, O. O.; Derry, M. J.; Doncom, K. E. B.; Rymaruk, M. J.; Armes, S. P. Polydimethylsiloxane-Based Diblock Copolymer Nano-objects Prepared in Nonpolar Media via RAFT-Mediated Polymerization-Induced Self-Assembly. *Macromolecules* **2015**, *48*, 3547-3555.

(90) Derry, M. J.; Mykhaylyk, O. O.; Armes, S. P. A Vesicle-to-Worm Transition Provides a New High-Temperature Oil Thickening Mechanism. *Angew Chem Int Ed* **2017**, *56*, 1746-1750.

(91) Beliciu, C. M.; Moraru, C. I. Effect of solvent and temperature on the size distribution of casein micelles measured by dynamic light scattering. *J. Dairy Sci.* **2009**, *92*, 1829-39.

(92) Michor, E. L.; Berg, J. C. Temperature Effects on Micelle Formation and Particle Charging with Span Surfactants in Apolar Media. *Langmuir* **2015**, *31*, 9602-9607.

(93) Bendedouch, D.; Chen, S. H.; Koehler, W. C. Structure of Ionic Micelles from Small Angle Neutron Scattering. *J. Phys. Chem.* **1983**, *87*, 153-159.

(94) Ratcliffe, L. P. D.; Derry, M. J.; Ianiro, A.; Tuinier, R.; Armes, S. P. A Single Thermoresponsive Diblock Copolymer Can Form Spheres, Worms or Vesicles in Aqueous Solution. *Angew. Chem.-Int. Edit.* **2019**, *58*, 18964-18970.

(95) Clarkson, C. G.; Lovett, J. R.; Madsen, J.; Armes, S. P.; Geoghegan, M. Characterization of Diblock Copolymer Order-Order Transitions in Semidilute Aqueous Solution Using Fluorescence Correlation Spectroscopy. *Macromol. Rapid Commun.* **2015**, *36*, 1572-1577.

(96) Pei, Y. W.; Dharsana, N. C.; Van Hensbergen, J. A.; Burford, R. P.; Roth, P. J.; Lowe, A. B. RAFT dispersion polymerization of 3-phenylpropyl methacrylate with poly 2-(dimethylamino)ethyl methacrylate macro-CTAs in ethanol and associated thermoreversible polymorphism. *Soft Matter* **2014**, *10*, 5787-5796.

(97) Blanazs, A.; Verber, R.; Mykhaylyk, O. O.; Ryan, A. J.; Heath, J. Z.; Douglas, C. W. I.; Armes, S. P. Sterilizable Gels from Thermoresponsive Block Copolymer Worms. *J. Am. Chem. Soc.* **2012**, *134*, 9741-9748.